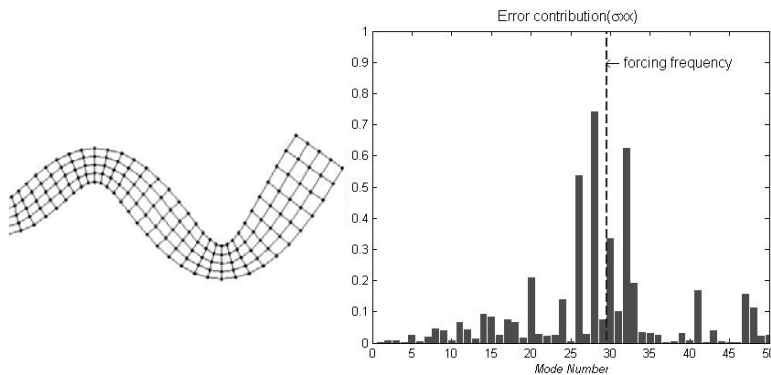


# Goal Oriented Estimation of Errors due to Modal Reduction in Dynamics



**Sandeep Shetty**

**Chukwudi Anthony Okeke**

Department of Mechanical Engineering  
Blekinge Institute of Technology  
Karlskrona, Sweden

2007

---

Supervisors: Ansel Berghuvud, Ph.D. Mech. Eng., BTH  
Kenneth Runnesson, Professor, Chalmers



# Goal Oriented Estimation of Error due to Modal Reduction in Dynamics

Shetty, Sandeep

Okeke, Chukwudi Anthony

Department of Mechanical Engineering

Blekinge Institute of Technology

Karlskrona, Sweden

2007

Thesis submitted for completion of Master of Science in Mechanical Engineering with emphasis on Structural Mechanics at the Department of Mechanical Engineering, Blekinge Institute of Technology, Karlskrona, Sweden.

## **Abstract:**

The aim of this thesis is the estimation of errors due to reduction in modal superposition method. Mode superposition methods are used to calculate the dynamic response of linear systems. In modal superposition method, it becomes unnecessary to consider all the modes of a particular system. In generally only a few number of modes contribute significantly to the solution. The main aim of the study is to identify the significant modes required for good approximation. Finally, this study constitutes a basis for developing an adaptive method, choosing the minimum number of modes required for certain accuracy. Procedure for evaluating errors is presented and numerical examples illustrate the behavior of the method in the context of forced harmonic response. Finite element modeling and simulation was carried out using MATLAB.

## **Keywords:**

Dynamic response, Mode superposition, Harmonic loads, Cantilever beam, Number of modes, Displacements, Stresses, Error estimation, Error contribution

# Acknowledgements

The thesis was carried out at the Applied Mechanics department of Chalmers University of Technology, under the supervision of Prof Kenneth Runnesson, Fredrik Larsson, and Torbjörn Ekevid (Växjö University).

We remain most grateful to all the supervisors for giving an idea and immense guidance during the thesis work. We thank Prof Kenneth Runnesson for kindly accepting us to do the thesis under his group and for his suggestion of the topic. We are equally grateful to Fredrick Larsson and Torbjörn Ekevid for guidance and valuable discussions throughout the thesis work.

We want to specially show our gratitude to our internal supervisor at BTH, Ansel Berghuvud for his professional advice, guidance and encouragement during the thesis work.

Finally, we want to thank all those who in one way or the other, contributed to the success of this thesis .We cannot, but remain indebted to you all.

Göteborg, January, 2007.

*Shetty, Sandeep*

*Okeke, Chukwudi Anthony*

# Contents

<b>1</b>	<b>Notation</b>	<b>5</b>
<b>2</b>	<b>Introduction</b>	<b>7</b>
<b>3</b>	<b>Theory</b>	<b>8</b>
3.1	Mode superposition method	8
3.2	The discrete system	8
3.3	Forced harmonic response	9
3.4	Undamped modal analysis	11
<b>4</b>	<b>Modal Synthesis for Forced Harmonic Response</b>	<b>12</b>
4.1	Complete basis-Diagonalization	12
4.2	Reduced basis-Diagonalization	14
<b>5</b>	<b>Error Analysis</b>	<b>17</b>
5.1	The residual and the error	17
5.2	Output functions	18
5.3	The error representation using a dual solution	18
5.4	Error contributions	19
<b>6</b>	<b>Simulation and results</b>	<b>21</b>
6.1	Numerical Example: Cantilever beam under harmonic load	21
6.2	Finite element model	22
6.3	Mode shapes	24
6.4	Displacement in X direction	25
6.4.1	Dual problem solution	25
6.4.2	Exact Error	26
6.4.3	Error estimation	27
6.4.4	Comparison-Estimated error v/s Exact error	29
6.4.5	Error Contribution	30
6.5	Displacement in Y direction	32
6.5.1	Dual problem solution	32
6.5.2	Exact Error	34
6.5.3	Error estimation	34
6.5.4	Error contribution	36
6.6	In plane stress $\sigma_{xx}$	37
6.6.1	Dual problem solution	37
6.6.2	Exact Error	39
6.6.3	Error estimation	39

6.6.4 Error contribution	41
<b>7 Discussions and conclusions</b>	<b>43</b>
<b>8 Future work</b>	<b>44</b>
<b>9 References</b>	<b>45</b>

# 1 Notation

$F$	Load	[N]
$L$	length of the cantilever beam	[m]
$B$	Beam's width	[m]
$H$	Height of the beam	[m]
$\rho$	Density	[kg/m <sup>3</sup> ]
$T$	Time duration	[sec]
$E$	Young's modulus	[N/m <sup>2</sup> ]
$I$	Moment of Inertia	[m <sup>4</sup> ]
$M$	Mass	[kg]
$\omega$	Angular frequency	[rad/s]
$F$	Frequency	[Hz]
$Y$	Displacement	[mm]
$\zeta$	Damping coefficient	
$U_x$	Displacement in x-direction	[mm]
$U_y$	Displacement in y-direction	[mm]
$\sigma_{xx}$	In plane stress in xx	[N/mm <sup>2</sup> ]
$\underline{M}$	Mass matrix	
$\underline{K}$	Stiffness matrix	
$\underline{C}$	Damping matrix	
$\underline{\tilde{f}}$	Modal load vector	
$\underline{\tilde{Z}}$	Modal dynamic stiffness matrix	
$\underline{\tilde{Z}}_R$	Reduced modal dynamic stiffness	
$\Phi$	Modal matrix	

$m_i$	Modal mass coefficient
$k_i$	Modal static stiffness
$\eta_i^*$	Dual mode amplitude
$e_i$	Modal error
$r_i$	Modal residual
$\omega_i$	Eigen frequencies
$\underline{\varphi}_i$	Eigen vector

## Abbreviations

FE	Finite element
MDOF	Multiple degree of freedom
SDOF	Single degree of freedom
DOF	Degree of freedom
2D	2 Dimensional

## 2 Introduction

Usually linear dynamic response problems are solved using mode superposition or direct integration schemes. Mode superposition, however, is a suitable method for calculating the dynamic stresses and displacements of complicated structures which are subjected to external excitations, where by only the excited displacement modes need to be accounted for. Today, mode superposition methods are extensively used in the analysis of complicated structures which are acted upon by various types of loads like earthquake acceleration, blast over pressures e.t.c.

Mode superposition uses the synthesis of the response as the eigenvectors weighted by the corresponding modal coordinates to calculate the structure's response. The eigenvector or eigenmodes are obtained from modal analysis. Mode superposition is most suitable for linear problems with long time duration. It requires fewer calculations than the full integration method, this is a faster and less expensive method.

In mode superposition it is not necessary to consider all the modes, but it is important to evaluate the natural frequencies above and below that of the analysis range. This is due to the fact that, in practice, there is never just one distinct mode of vibration due to an excitation, but one dominant mode with a range of additional harmonics from the adjacent upper and lower modes. It is important to note that it is not merely the eigenfrequency of a mode that governs whether or not it will be significant. In fact this is the fundamental rationale for developing the method to be presented in this thesis.

The main objective of this thesis is the application of estimation of errors due to modal reduction in the modal superposition method. Such estimation leads to general indicators that identify rules of significance.

# 3 Theory

## 3.1 Mode superposition method

Mode superposition method uses free vibration mode shape amplitudes for calculation of displacements. They describe the displacements efficiently and their orthogonal properties make good approximation with few terms.

The mode superposition method, simply put, is used for calculation of the dynamic response of a system by uncoupling the system of equations of motion, to get an independent SDOF equation for each mode of vibration. So that the dynamic response can be found separately for each modal coordinate and then superimposing these for all significant modes to obtain the response in original coordinates.

(Clough and Penzien,1993) maintain that the normal co-ordinate transformation which serves to change the set of coupled equations of motions of a MDOF system into a set of N uncoupled equations ,is the basis for the mode superposition method. However, its worthy of note to know that after the transformation the equations are solved either by a step-by-step integration in the time domain or by the use of the frequency domain methods.

## 3.2 The discrete system

We shall consider a dynamic system, discretized in space that can be described by the linear equations of motions as

$$\underline{M}\ddot{x} + \underline{C}\dot{x} + \underline{K}x = f \quad (3.1)$$

Where  $\underline{x}$  is a vector of size  $(nx1)$  containing the unknown displacements of the system. Furthermore,  $\underline{M}$ ,  $\underline{C}$  and  $\underline{K}$  are the system matrices of size  $(n \times n)$ : the mass, damping and stiffness matrices, respectively. External forces are applied in terms of the load vector  $f$  of size  $(n \times n)$ . Time derivatives are denoted as follows:

$$\underline{\dot{x}} \stackrel{\text{def}}{=} \frac{d}{dt} \underline{x}, \quad \underline{\ddot{x}} \stackrel{\text{def}}{=} \frac{d^2}{dt^2} \underline{x} \quad (3.2)$$

In order to solve (3.1) during a period of time, for  $0 < t \leq T$ , we need to give the data to the problem in terms of the loading  $f(t)$  for  $0 < t \leq T$ , as well as the initial conditions  $\underline{x}(0)$  and  $\underline{\dot{x}}(0)$ .

### 3.3 Forced harmonic response

We shall now study the stationary response due to a harmonic loading

$$\underline{f}(t) = \underline{\hat{f}} \cos(\omega t) = \text{Re} \left\{ \underline{\hat{f}} e^{i\omega t} \right\} \quad (3.3)$$

Where  $\underline{\hat{f}}$  the real-valued amplitude of the applied load and  $\omega$  is the forcing frequency. Neglecting all transient effects, we assume that the response can be described as a harmonic function of the same frequency, i.e we make the anzats

$$\underline{x}(t) = \text{Re} \left\{ \underline{\hat{x}} e^{i\omega t} \right\} \quad (3.4)$$

Using (3.3) and (3.4) in (3.1), we may state that

$$\text{Re} \left\{ \underline{M} \frac{d^2}{dt^2} (\underline{\hat{x}} e^{i\omega t}) + \underline{C} \frac{d}{dt} (\underline{\hat{x}} e^{i\omega t}) + \underline{K} (\underline{\hat{x}} e^{i\omega t}) \right\} = \text{Re} \left\{ \underline{\hat{f}} e^{i\omega t} \right\} \quad (3.5)$$

Where we used that  $\frac{d}{dt} (\text{Re}\{a(t)\}) = \text{Re} \left\{ \frac{d}{dt} (a(t)) \right\}$  for a complex function  $a(t)$ , and the fact that  $\underline{M}$ ,  $\underline{C}$ ,  $\underline{K}$  are real-valued matrices.

Since the amplitude  $\underline{\hat{x}}$  is a constant, although possibly complex, we may evaluate the time-derivatives as follows:

$$\frac{d}{dt}(\hat{x}e^{i\omega t}) = \hat{x} \frac{d}{dt}e^{i\omega t} = i\omega \hat{x}e^{i\omega t}, \quad \frac{d^2}{dt^2}(\hat{x}e^{i\omega t}) = -\omega^2 \hat{x}e^{i\omega t} \quad (3.6)$$

Inserting these results into(3.5), we obtain

$$\text{Re}\{(-\omega^2 \underline{M} + i\omega \underline{C} + \underline{K}) \hat{x} e^{i\omega t}\} = \text{Re}\left\{ \underline{f} e^{i\omega t} \right\} \quad (3.7)$$

In(3.7),we identify that we have  $n$  equations but  $2n$  unknowns ,since the equation is real-valued and the unknown,  $\hat{x}$ ,is complex. The next step is thus to use the fact that the expressions are harmonic and that, for any complex and harmonic function  $A = \hat{A}e^{i\omega t}$

$$\begin{aligned} \frac{d}{dt} \text{Re}\{A(t)\} &= \frac{d}{dt} \text{Re}\left\{ \hat{A} e^{i\omega t} \right\} = \text{Re}\left\{ \frac{d}{dt} (\hat{A} e^{i\omega t}) \right\} = \text{Re}\left\{ i\omega \hat{A} e^{i\omega t} \right\} \\ &= \omega \text{Re}(iA(t)) = -\omega \text{Im}\{A(t)\} \end{aligned} \quad (3.8)$$

We may thus express the time derivative of (3-7) as

$$-\omega \text{Im}\left\{ -\omega^2 \underline{M} + i\omega \underline{C} + \underline{K} \right\} \hat{x} e^{i\omega t} = -\omega \text{Im}(\underline{f} e^{i\omega t}) \quad (3.9)$$

Clearly, combining (3-13) and (3-15) gives the complex-valued equation,

$$(-\omega^2 \underline{M} + i\omega \underline{C} + \underline{K}) \hat{x} e^{i\omega t} = \underline{f} e^{i\omega t} \quad (3.10)$$

Finally, since the time-dependent term  $e^{i\omega t}$  appears on both sides, we may state the equations for the forced harmonic response as

$$\left( -\omega^2 \underline{M} + i\omega \underline{C} + \underline{K} \right) \hat{x} = \underline{f} \quad (3.11)$$

This can be abbreviated as

$$\underline{Z}(\omega) \hat{x} = \underline{f}, \quad \underline{Z}(\omega) \stackrel{\text{def}}{=} -\omega^2 \underline{M} + i\omega \underline{C} + \underline{K} \quad (3.12)$$

Where  $\underline{Z}(\omega)$  is the frequency-dependent *dynamic stiffness matrix*.

Note that (3.10) resembles a static problem, where  $\hat{x}$  is the complete amplitudes of the response for any given forcing frequency  $\omega$ .

### 3.4 Undamped modal analysis

For the undamped system, obtained by setting  $\underline{C} = \underline{0}$ , we may study the resonance problem defined by sustained vibration without any external loading. In terms of the forced harmonic response (3.9), we may express the resonance problem as

$$(\underline{K} - \omega^2 \underline{M})\underline{\varphi} = \underline{0} \tag{3.13}$$

This is an eigenproblem with solutions  $w_i$  and  $\varphi_i$  that satisfy

$$(\underline{K} - \omega_i^2 \underline{M})\underline{\varphi}_i = \underline{0}, i = 1, 2, \dots, n \tag{3.14}$$

Where  $w_i$  are the eigenfrequencies and  $\underline{\varphi}_i$  is the mode shape (eigenvector) pertinent to the eigenvalue  $w_i$ . Note that each  $\underline{\varphi}_i$  has the shape of displacement amplitude, and thus is of size  $(n \times 1)$ . Furthermore, since the eigenvalue problem (3.13) is solved for the undamped case,  $\{\underline{\varphi}_i\}$  are real-valued.

Finally, we note that the amplitude of the mode-shapes is undetermined, i.e. we may express  $\underline{\varphi}_i$  as  $\underline{\varphi}_i = \alpha \underline{\varphi}_i^{computed}$  with an arbitrary  $\alpha \neq 0$ , where  $\underline{\varphi}_i^{computed}$  is one solution pertinent to  $\omega_i$ .

# 4 Modal Synthesis for Forced Harmonic Response

## 4.1 Complete basis-Diagonalization

It can be shown that the eigenmodes  $\{\underline{\varphi}_i\}_{i=1}^n$  constitute a basis for  $R^n$ , and thus any amplitude can be written as

$$\hat{\underline{x}} = \sum_{i=1}^n \underline{\varphi}_i \eta_i = \underline{\Phi} \underline{\eta} \quad (4.1)$$

Where we introduced the modal matrix  $\underline{\Phi}$  of size  $(n \times n)$  and the (complex) modal coordinates  $\eta_i$  collected in the vector  $\underline{\eta}$  of size  $(n \times 1)$  as follows:

$$\underline{\Phi} = [\underline{\varphi}_1, \underline{\varphi}_2, \dots, \underline{\varphi}_n] \quad , \underline{\eta} = [\eta_1, \eta_2, \dots, \eta_n]^T \quad (4.2)$$

Upon introducing the expression for  $\hat{\underline{x}}$  in (4.1) and pre-multiplying by  $\underline{\Phi}^T$ , we obtain from (3.12) that

$$\tilde{\underline{Z}}(\omega) \underline{\eta} = \tilde{\underline{f}} \quad (4.3)$$

Where  $\tilde{\underline{Z}}$  is the modal dynamic stiffness matrix

$$\tilde{\underline{Z}}(\omega) \stackrel{def}{=} \underline{\Phi}^T \underline{Z}(\omega) \underline{\Phi} = -\omega^2 \tilde{\underline{M}} + i\omega \tilde{\underline{C}} + \tilde{\underline{K}} \quad (4.4)$$

With

$$\tilde{\underline{M}} \stackrel{def}{=} \underline{\Phi}^T \underline{M} \underline{\Phi}, \quad \tilde{\underline{C}} \stackrel{def}{=} \underline{\Phi}^T \underline{C} \underline{\Phi}, \quad \tilde{\underline{K}} \stackrel{def}{=} \underline{\Phi}^T \underline{K} \underline{\Phi} \quad (4.5)$$

And where  $\tilde{\underline{f}}$  is the modal load vector.

$$\tilde{\underline{f}} \stackrel{def}{=} \underline{\Phi}^T \underline{f} \quad (4.6)$$

It follows from the orthogonality properties of the eigenvalue problem that  $\tilde{\underline{M}}$  and  $\tilde{\underline{K}}$  are diagonal matrices hence,

$$\underline{\tilde{M}} = \underline{\Phi}^T \underline{M} \underline{\Phi} = \begin{bmatrix} m_1 & & \\ & m_2 & \\ & & m_n \end{bmatrix}, \quad m_i \stackrel{def}{=} \underline{\varphi}_i^T \underline{M} \underline{\varphi}_i \quad (4.7)$$

$$\underline{\tilde{K}} = \underline{\Phi}^T \underline{K} \underline{\Phi} = \begin{bmatrix} k_1 & & \\ & k_2 & \\ & & k_3 \end{bmatrix}, \quad k_i \stackrel{def}{=} \underline{\varphi}_i^T \underline{K} \underline{\varphi}_i \quad (4.8)$$

Here, we introduced the modal mass coefficients,  $m_i$ , and the modal static stiffness coefficients,  $k_i$ . From (3.14), the eigenvalues can be computed as

$$\omega_i^2 = \frac{k_i}{m_i} \quad (4.9)$$

Furthermore, in this section we shall assume that the damping matrix has a certain format, such that  $\underline{\tilde{C}}$  becomes diagonal as well, i.e.,

$$\underline{\tilde{C}} = \underline{\Phi}^T \underline{C} \underline{\Phi} = \begin{bmatrix} c_1 & & \\ & c_2 & \\ & & c_n \end{bmatrix}, \quad c_i \stackrel{def}{=} \underline{\varphi}_i^T \underline{C} \underline{\varphi}_i \quad (4.10)$$

Whereby the coefficients  $c_i$  denotes the modal damping coefficients. This is the case, for instance, if we choose a proportional damping, defined by  $\underline{C} = \alpha \underline{M} + \beta \underline{K}$ , where  $\alpha$  and  $\beta$  are real valued coefficients.

Moreover,  $\underline{\tilde{f}}$  is the vector of modal loading coefficients

$$\underline{\tilde{f}} = \underline{\Phi}^T \underline{f} = \begin{bmatrix} \tilde{f}_1 \\ \tilde{f}_2 \\ \cdot \\ \cdot \\ \tilde{f}_n \end{bmatrix}, \quad \tilde{f}_i \stackrel{def}{=} \underline{\varphi}_i^T \underline{f}, \quad (4.11)$$

We are now in the position to formulate the uncoupled modal equations from (4.3) as

$$z_i(\omega)\eta_i = \tilde{f}_i \text{ where } i = 1, \dots, n \Rightarrow \frac{\tilde{f}_i}{Z_i(\omega)} \quad (4.12)$$

Where, we introduced the modal dynamic stiffness coefficients

$$z_i(\omega) \stackrel{\text{def}}{=} -\omega^2 m_i + i\omega c_i + k_i \quad (4.13)$$

As an alternative, we may express  $Z_i(\omega)$  as

$$z_i(\omega) = m_i(-\omega^2 + 2i\zeta_i\omega_i\omega + \omega_i^2), \quad \zeta_i \stackrel{\text{def}}{=} \frac{c_i}{2\omega_i}, \quad i = 1, \dots, n \quad (4.14)$$

Where the coefficients  $\zeta_i$  represent the relative modal damping,

To sum up, the solution to (3.12) can thus be obtained as follows:

- Solve for  $\eta_i$  from (4.12) for each mode,  $i = 1, 2, \dots, n$
- Add up contributions from each mode to give  $\hat{x}$  from (4.1) ,i.e.

$$\hat{x} = \underline{\Phi}\underline{\eta} = \sum_{i=1}^n \underline{\varphi}_i \eta_i \quad (4.15)$$

## 4.2 Reduced basis-Diagonalization

In order to reduce the computational effort, we now consider only a set of  $m \leq n$  modes  $M$ . An appropriate solution (3.12) is thus sought as the linear combination

$$\hat{x} \cong \hat{x}_R = \sum_{i \in M} \underline{\varphi}_i \eta_{R,i} = \underline{\Phi}_R \underline{\eta}_R \quad (4.16)$$

Where  $\underline{\Phi}_R$  is of size  $(n \times m)$  and contains the reduced basis modes, while  $\underline{\eta}_R$  contains the corresponding modal amplitudes.

It is common practice to choose the first consecutive modes in  $M$ , i.e.  $M = \{1, 2, \dots, m\}$ .

However, such a choice is by no means necessary (or even desirable) in general.

Upon inserting (4.16) in (3.12) and pre-multiplying by  $\underline{\Phi}_R^T$ , we obtain

$$\tilde{\underline{Z}}_R(\omega)\underline{\eta}_R = \underline{\hat{f}}_R \quad (4.17)$$

Where  $\tilde{\underline{Z}}_R$  is the reduced modal dynamic stiffness matrix

$$\tilde{\underline{Z}}_R(\omega) \stackrel{def}{=} \underline{\Phi}_R^T \underline{Z}(\omega) \underline{\Phi} - \omega^2 \tilde{\underline{M}}_R + i\omega \tilde{\underline{C}}_R + \tilde{\underline{K}}_R \quad (4.18)$$

With

$$\tilde{\underline{M}}_R \stackrel{def}{=} \underline{\Phi}_R^T \underline{M} \underline{\Phi}_R, \quad \tilde{\underline{C}}_R \stackrel{def}{=} \underline{\Phi}_R^T \underline{C} \underline{\Phi}_R, \quad \tilde{\underline{K}}_R \stackrel{def}{=} \underline{\Phi}_R^T \underline{K} \underline{\Phi}_R \quad (4.19)$$

And where

$$\underline{\hat{f}}_R \stackrel{def}{=} \underline{\Phi}_R^T \hat{\underline{f}} \quad (4.20)$$

Again, it follows from the orthogonality properties of the eigenmodes that  $\tilde{\underline{M}}_R$  and  $\tilde{\underline{K}}_R$  are diagonal matrices

$$\tilde{\underline{M}}_R = \underline{\Phi}_R^T \underline{M} \underline{\Phi}_R = \begin{bmatrix} m_1 & & \\ & m_2 & \\ & & \ddots \\ & & & m_m \end{bmatrix} \quad (4.21)$$

$$\tilde{\underline{K}}_R = \underline{\Phi}_R^T \underline{K} \underline{\Phi}_R = \begin{bmatrix} k_1 & & \\ & k_2 & \\ & & \ddots \\ & & & k_m \end{bmatrix} \quad (4.22)$$

and under the same assumptions leading to (4.9), we conclude that  $\tilde{\underline{C}}_R$  is also diagonal, i.e.

$$\tilde{\underline{C}}_R = \underline{\Phi}_R^T \underline{C} \underline{\Phi}_R = \begin{bmatrix} c_1 & & \\ & c_2 & \\ & & \ddots \\ & & & c_m \end{bmatrix} \quad (4.23)$$

Finally, we conclude that,

$$\underline{\tilde{f}}_R = \underline{\Phi}_R^T \underline{\tilde{f}} = \begin{bmatrix} \tilde{f}_1 \\ \tilde{f}_2 \\ \cdot \\ \cdot \\ \tilde{f}_m \end{bmatrix}, \quad \tilde{f}_i \stackrel{def}{=} \underline{\varphi}_i^T \underline{\hat{f}} \quad (4.24)$$

It is of considerable interest to note that  $(\underline{\tilde{f}}_R)_i = (\underline{\tilde{f}})_i$  for  $i \in M$ . Under the same assumption as those leading to (4.12), we thus obtain  $m$  decoupled equations from (4.17)

$$z_i(\omega)\eta_{R,i} = \tilde{f}_i, \quad i \in M \quad (4.25)$$

and, upon comparing with the unreduced equations in (4.12), it follows readily that

$$\eta_{R,i} = \eta_i \quad \text{for } i \in M. \quad (4.26)$$

Hence, we conclude that the reduced basis expansion in (4.17), which is due to the orthogonality properties of the modes  $\underline{\varphi}_i$ .

**Remark:** In a more general situation the orthogonality properties do not apply, and all the modal coordinates change when the basis is changed. Important examples are (i) non-proportional damping where  $\underline{\Phi}^T \underline{C} \underline{\Phi}$  is non-diagonal, (ii) nonlinearity is present or (iii) a non-diagonal reduction method (such as Craig-Bampton method) is employed. The last situation is studied in further detail subsequently.

# 5 Error Analysis

## 5.1 The residual and the error

The approximation  $\hat{\underline{x}}_R \cong \hat{\underline{x}}$  will not satisfy the original equation(3.12), exactly but will produce a residual

$$\underline{\hat{r}} \stackrel{def}{=} \underline{\hat{f}} - \underline{Z}(\omega)\hat{\underline{x}}_R. \quad (5.1)$$

The *modal residual* is given as

$$\tilde{r}_i \stackrel{def}{=} \underline{\varphi}_i^T \underline{\hat{r}} = \underline{\varphi}_i^T (\underline{\hat{f}} - \underline{Z}(\omega)\hat{\underline{x}}_R) = \tilde{f}_i - \sum_{j \in M} z_{ij}(\omega)\eta_{R,j} \quad (5.2)$$

and we conclude that

$$\begin{aligned} \tilde{r}_i &= 0 \quad \text{if } i \in M \\ \tilde{r}_i &= 0 \quad \text{if } i \notin M \end{aligned} \quad (5.3)$$

Hence,  $\tilde{r}_i = 0$  when  $\underline{\varphi}_i$  is part of the reduced basis. In the special case that  $z_{ij}$  is diagonal then it follows that

$$\tilde{r}_i = \tilde{f}_i \quad \text{if } i \notin M \quad (5.4)$$

when it is said that  $z_{ij} = 0$  for  $i \notin M$  and  $j \in M$ .

It is noted the residual is directly computable for any given approximation  $\hat{\underline{x}}_R$ . However, we would like to assess the (influence of) the error

$$\underline{\hat{e}} \stackrel{def}{=} \hat{\underline{x}} - \hat{\underline{x}}_R \quad (5.5)$$

which is not directly computable, since it does require the exact solution  $\hat{\underline{x}}_R$  !.

## 5.2 Output functions

In engineering practice the goal of the analysis is to compute a specific output (of engineering interest). Examples of such outputs are amplitudes of displacements, stresses, e.t.c. We shall, consider a goal-oriented error analysis with the purpose to quality and control the error in the chosen output(s).

Henceforth, we shall restrict ourselves to study only linear outputs, in which case the output quantity,  $Q(\hat{x})$  can be expressed as

$$Q(\hat{x}) = \underline{q}^T \hat{x} \quad (5.6)$$

where  $\underline{q}$  is given (a priori chosen) vector of size (nx1); the extraction function. For an approximation  $\hat{x}_R$ , we can thus compute the approximate value of the output as

$$Q_R \stackrel{def}{=} Q(\hat{x}_R) = \underline{q}^T \hat{x}_R \quad (5.7)$$

## 5.3 The error representation using a dual solution

Our goal is now to study the error in the output function

$$E = Q(\hat{x}) - Q(\hat{x}_R) = Q(\hat{e}) \quad (5.8)$$

where we used the linearity of  $Q$ . The idea is to establish a relation  $E$  and to make the residual computable. To this end, we establish the *dual problem*

$\underline{Z}(\omega)^T \hat{x}^* = \underline{q}$  where  $\hat{x}_R^*$  is a vector of size (nx1), and the loading is described by the output quantity via (5.2).

**Remark:** Note that the dynamic stiffness matrix  $Z(\omega)$  is symmetric, and thus, (5.5) can be recast as  $\underline{Z}(\omega)\hat{x}^* = \underline{q}$ .

Using the dual solution  $\hat{x}^*$ , we may proceed from (5.4) as follows

$$\begin{aligned} E &= \underline{q}^T \hat{e} = \{(5.5)\} = (\hat{x}^*)^T \underline{Z}(\omega) \hat{e} \\ &= \{(5.1)\} = (\hat{x}^*)^T \underline{Z}(\omega) (\hat{x} - \hat{x}_R) \end{aligned} \quad (5.10)$$

Finally, using the original equation (3.12) and the definition of the residual in (4.27), we obtain from (5.6) the computable error representation

$$E = (\hat{\underline{x}}^*)^T \hat{\underline{r}} \quad (5.11)$$

We are thus in the position to compute the exact error  $E$  if we compute the exact dual solution  $\hat{\underline{x}}_R^*$ .

## 5.4 Error contributions

In order to develop adaptive algorithms we want not only to estimate the error but also determine from which (removed) mode the error contributions stem from. To this end, we make a modal decomposition of the dual solution as,

$$\hat{\underline{x}}^* = \sum_{i=1}^n \underline{\varphi}_i \eta_i^* = \underline{\Phi} \underline{\eta}^* \quad (5.12)$$

Introducing (5.8) into (5.7), we obtain

$$E = (\hat{\underline{x}}^*)^T \hat{\underline{r}} = (\underline{\eta}^*)^T \underline{\Phi}^T \hat{\underline{r}} = \sum_{i=1}^n \eta_i^* \tilde{r}_i = \sum_{i=1}^n e_i \quad (5.13)$$

where  $\eta_i^*$  is the *dual mode amplitude* and  $e_i = \eta_i^* \tilde{r}_i$  is the modal error, where the modal residual  $r_i$  was defined in (4.28). However, since  $\tilde{r}_i = 0$  when  $i \in M$ , we will get contributions to the error on  $Q$  only from those modes that are *not part of the reduced basis*, such that we may rewrite (5.9) as

$$E = \sum_{i \notin M} e_i \quad (5.14)$$

This conclusion holds also if the dual solution is approximated using a suitably reduced basis. The most straightforward is defined as

$$\underline{\hat{x}}^* \cong \underline{\hat{x}}_R^* = \sum_{i=M^+} \underline{\varphi}_i \eta_{R,i}^{*(+)} = \underline{\Phi}_{R,}^{(+)} \underline{\eta}_R^{*(+)}$$

(5.15)

where  $M^{(+)} = \{1, 2, \dots, m, m+1\}$

# 6 Simulation and results

The procedure for evaluating errors is presented using the following numerical example with different combination of inputs and outputs.

## 6.1 Numerical Example: Cantilever beam under harmonic load

A cantilever beam as shown in fig6.1 is used as a basic structure for evaluating errors. Angular Harmonic load (7000N) is used to excite the structure. Load is applied at free end of the beam at an angle of 45 degree to y axis.

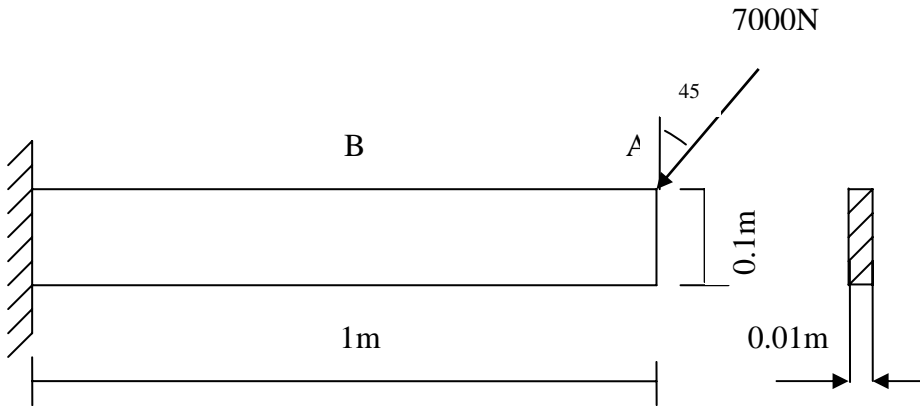


Figure 6.1. Cantilever beam under harmonic load.

Material properties of the beam:

Young's modulus  $E=210e9Gpa$

Poisson's ratio  $\gamma=0.3$

Density  $\rho=7800kg/m^3$

Three excitation frequencies and three output functions were used for evaluation. These are shown in tables 6.1 and 6.2.

*Table 6.1. Forcing frequencies.*

Forcing frequencies		
F1	F2	F3
800Hz	22500Hz	44500Hz

*Table 6.2. Output functions.*

Out put functions		
U <sub>x</sub> (Displacement in x direction at A)	U <sub>y</sub> (Displacement in y direction at A)	$\sigma_{.xx}$ (Inplane stress at point B)

## 6.2 Finite element model

The cantilever beam is modelled with *isoparametric* four-node quadrilateral plane-stress finite element. Each node has 2 degrees of freedom.

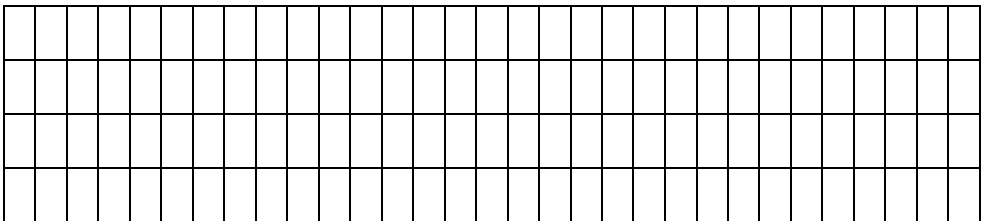


*Figure 6.2. Finite element model.*

The model contains 330 degrees of freedom in total out of which 10 degrees of freedom are constrained.

### Isoparametric elements:

Isoparametric formulation permits quadrilateral elements to have non rectangular shapes, which is achieved from transformation of the parent domain known as the  $\xi\eta$ -coordinate system to the global domain, called the xy-coordinate system.

### Plane stress elements

The plane stress assumptions states that only in plane stress components are non-zero i.e. that of transverse stresses are negligible

### Integration scheme

Integration of membrane strain terms was done using gauss integration, 9 integration points.

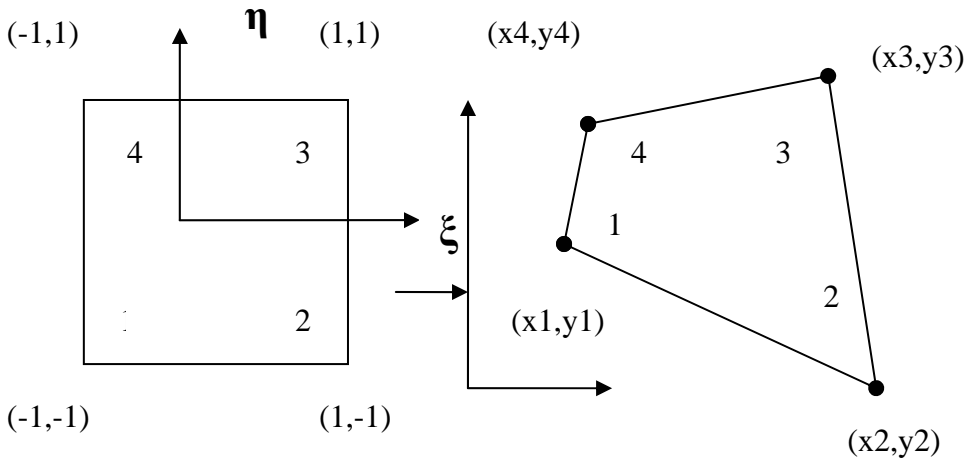


Figure 6.3. Mapping into four node isoparametric quad element from the parent domain to global.

## 6.3 Mode shapes

Since all calculations in mode superposition are based on modal amplitude, in figure 6.4 we have plotted six of the initial mode shapes of the structure.



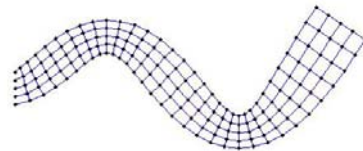
a) Mode 1,  $f_1 = 90$  Hz



b) Mode 2,  $f_2 = 510$  Hz



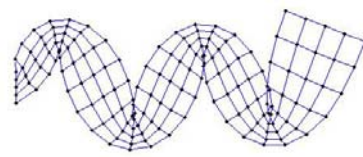
c) Mode 3,  $f_3 = 1300$  Hz



d) Mode 4,  $f_4 = 1350$  Hz



e) Mode 5,  $f_5 = 2470$  Hz



f) Mode 6,  $f_6 = 3800$  Hz

Figure 6.4. Mode shapes.

## 6.4 Displacement in X direction

Here we study the errors in calculation displacement in  $x$  direction. Output is at the free end of the beam. All the results presented are in  $mm$ .

### 6.4.1 Dual problem solution

As stated in the theory above we now start with dual solution problem. Here dual displacements were calculated for different forcing frequencies, and deformed shape of beam is plotted. Figures were scaled accordingly.

From equation (5.9) we can write the *dual problem* as

$$\underline{Z}(\omega^T) \hat{\underline{x}}^* = \underline{q} \quad (6.1)$$

Where  $\hat{\underline{x}}^*$  vector of size is  $(n \times 1)$  represents the dual displacement,  $\underline{q}$  is the  $q$  vector generated for *output*  $Ux$  (tip displacement in  $x$  direction). The dual displacement is shown in figures 6.5-6.7 for three forcing frequencies.

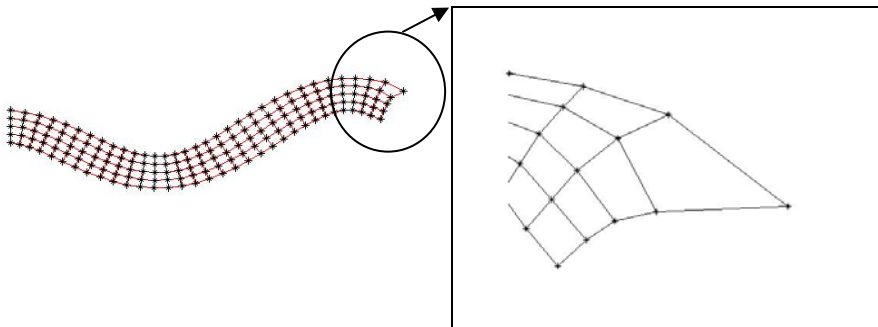


Figure 6.5. Dual displacement  $Re \{ \hat{\underline{x}}^* \}$ ,  $f = 800$  Hz.

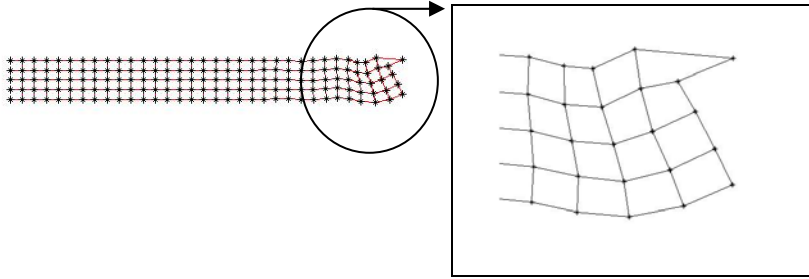


Figure 6.6. Dual displacement  $Re \{ \hat{x}^* \}$ ,  $f = 22500$  Hz.

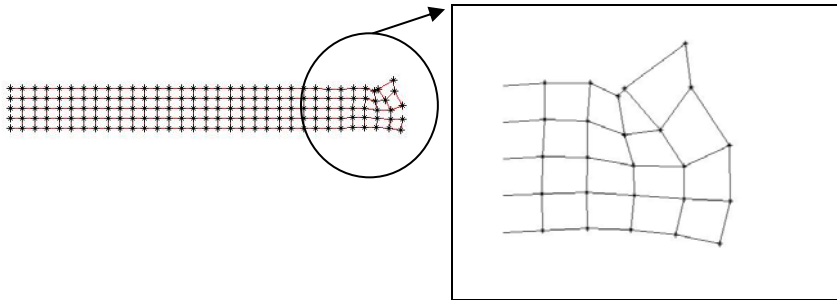


Figure 6.7. Dual displacement  $Re \{ \hat{x}^* \}$ ,  $f = 44500$  Hz.

## 6.4.2 Exact Error

Here exact error was calculated with the number of modes. Displacement which is calculated using all modes was considered as exact solution. Exact error was calculated taking difference between exact solution and the solution by using reduced number of modes. And exact error was plotted against the modes.

Using (5.8) we can write the *exact* error

$$E = Q(\hat{x}) - Q(\hat{x}_R) = Q(\hat{e}) \quad (6.2)$$

### 6.4.3 Error estimation

Error estimation was done using the procedure as explained in theory part, this is done by using dual modal solution and residues. Comparison was done between the exact error and the estimated error.

Using (5.13) we can write the *estimated* error

$$E = (\hat{\underline{x}}^*)^T \hat{\underline{r}} = (\underline{n}^*)^T \underline{\phi}^T \hat{\underline{r}} = \sum_{i=1}^n n_i^* \tilde{r}_i = \sum_{i=1}^n e_i \quad (6.3)$$

Since  $\tilde{r}_i = 0$  when  $i \in M$

$$E = \sum_{M+1}^n e_i \quad (6.4)$$

Exact error in calculating  $u_x$  is plotted in figures 6.8-6.10 for three different forcing frequencies. The relative error is defined as

$$\text{Relative error Er} = \frac{Q(\hat{\underline{x}}) - Q(\underline{x}_R)}{Q(\hat{\underline{x}})}$$

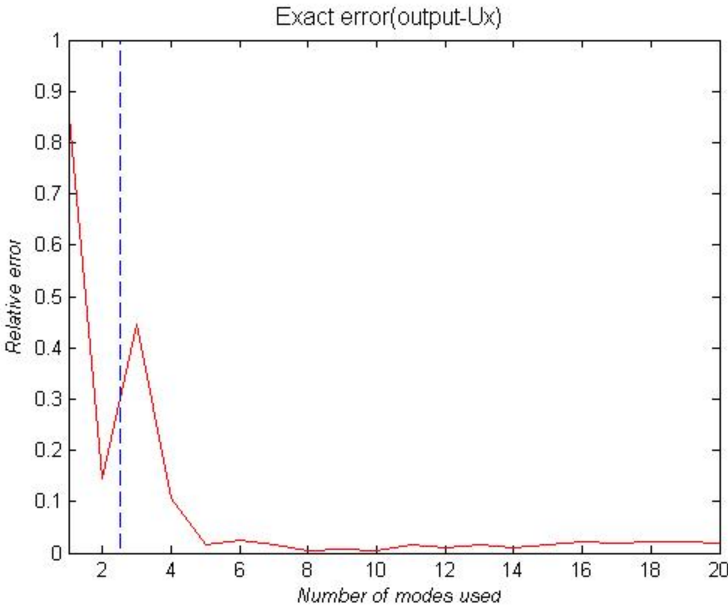


Figure 6.8. Exact error with number of modes,  $f = 800$  Hz, Output- $U_x$ .

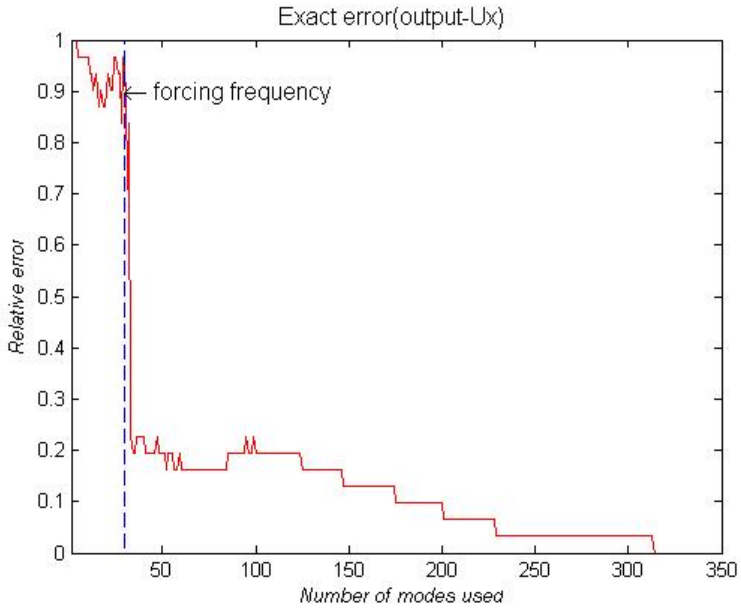


Figure 6.9. Exact error with number of modes,  $f = 22500$  Hz, Output- $U_x$ .

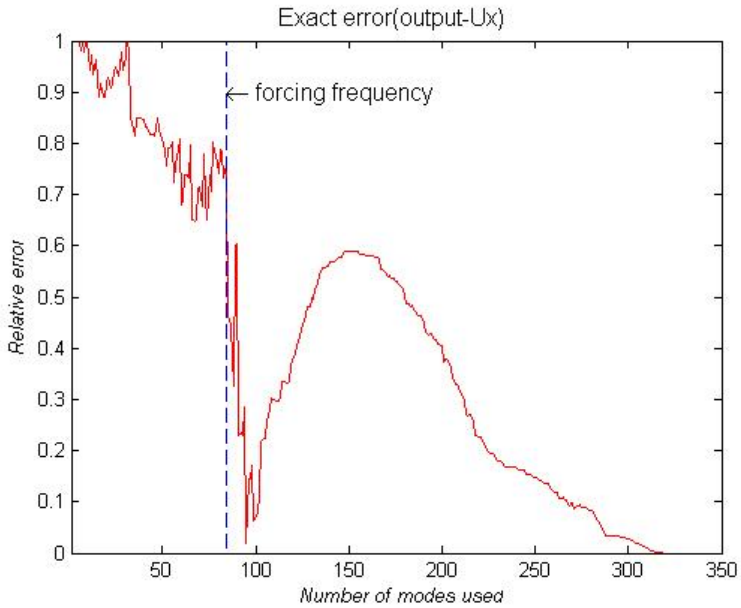


Figure 6.10. Exact error with number of modes,  $f = 44500$  Hz, Output- $U_x$ .

#### 6.4.4 Comparison-Estimated error v/s Exact error

A comparison of the estimated and the exact error is shown in figures 6.11-6.13.



Figure 6.11. Estimated/Exact error,  $f = 800$  Hz, output  $U_x$ .

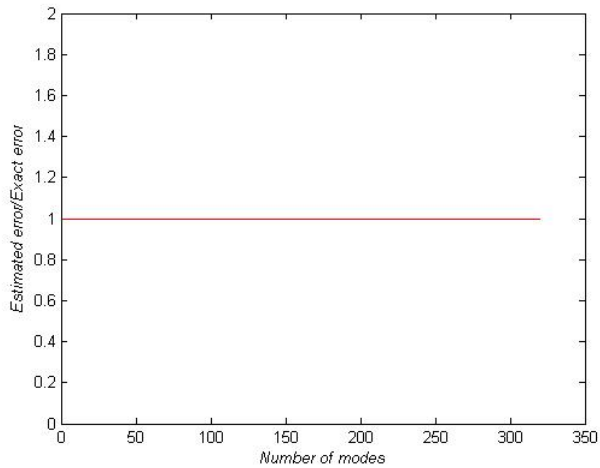


Figure 6.12. Estimated/Exact error,  $f = 22500$  Hz, output  $U_x$ .

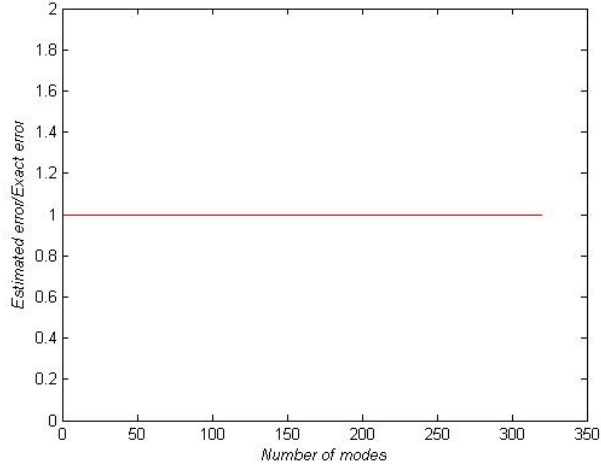


Figure 6.13. Estimated/Exact error,  $f = 44500$  Hz, output  $U_x$ .

#### 6.4.5 Error Contribution

Here, the error contribution by each mode is calculated using the same formula of error estimation, setting  $M=0$

Estimated error is written as

$$E = \sum_{M+1}^n e_i$$

By setting  $M=0$  in the above equation, we can calculate the *error contribution* by each mode.

$$\text{Relative error} = \frac{e_i}{Q(\hat{x})}$$

The estimated error contribution is shown in figures 6.14-6.16.

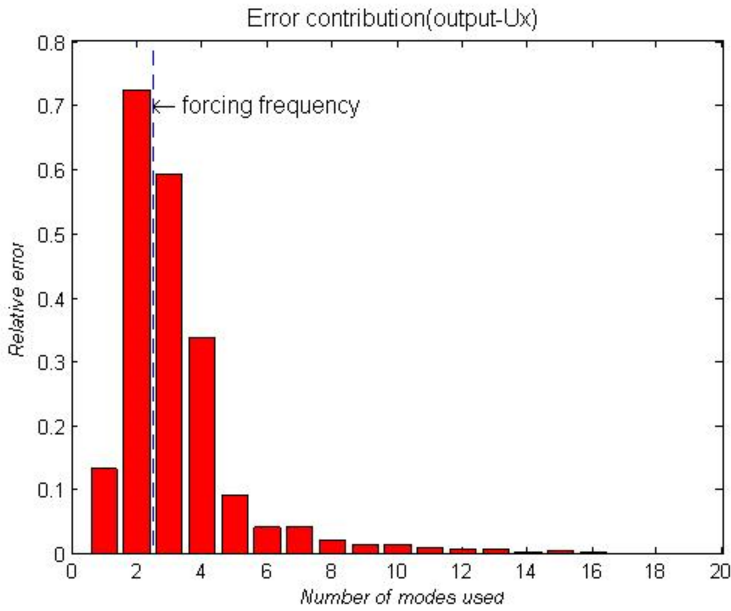


Figure 6.14. Estimated error contribution,  $f = 800$  Hz, output  $U_x$ .

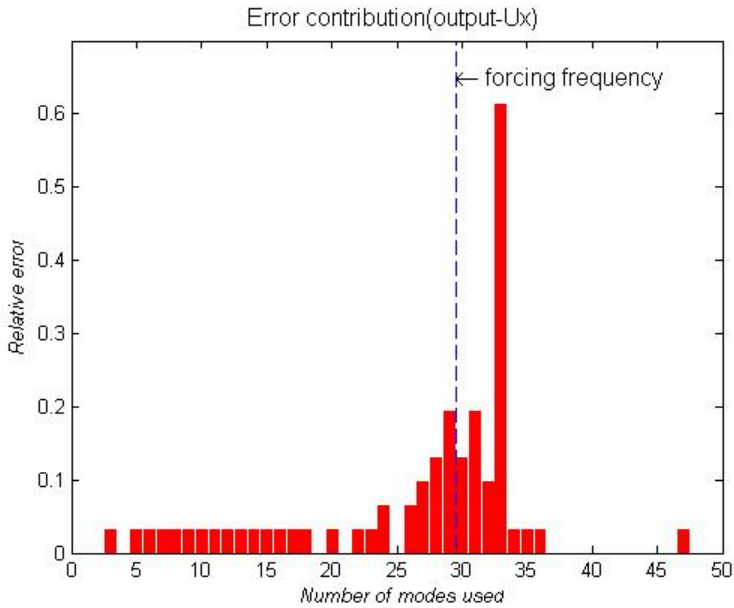


Figure 6.15. Estimated error contribution,  $f = 22500$  Hz, output  $U_x$ .

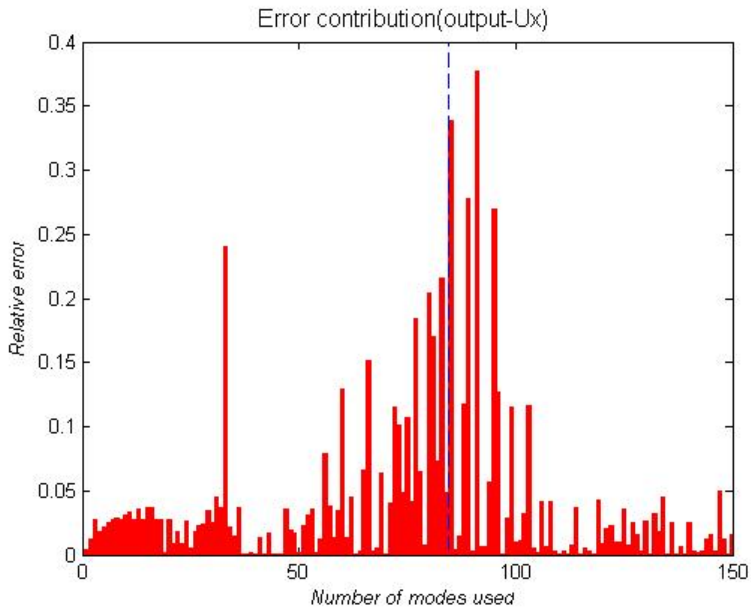


Figure 6.16. Estimated error contribution,  $f = 44500$  Hz, output  $U_x$ .

## 6.5 Displacement in Y direction

Here we study the errors in calculation displacement in y direction. Output point is at the free end of the beam. All the results presented are in *mm*. All the calculation which were done in chapter 6.4 are repeated here for the displacement output  $U_y$ .

### 6.5.1 Dual problem solution

Dual problem solution was done same as above case. The only change is  $\underline{q}$  vector generated for output  $U_y$ . Dual displacement is shown in figures 6.17-6.19 for three forcing frequencies.

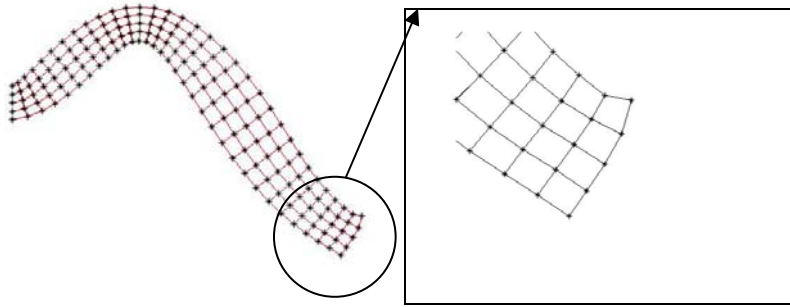


Figure 6.17. Dual displacement  $Re \{ \hat{x}^* \}$ ,  $f = 800$  Hz.

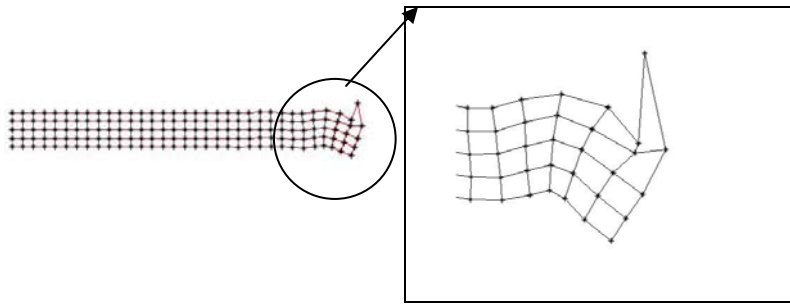


Figure 6.18. Dual displacement  $Re \{ \hat{x}^* \}$ ,  $f = 22500$  Hz.

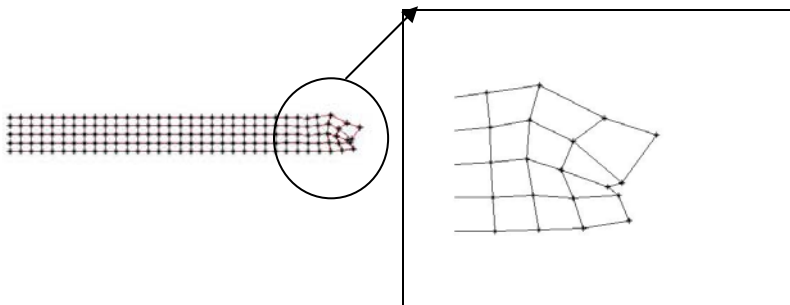


Figure 6.19. Dual displacement  $Re \{ \hat{x}^* \}$ ,  $f = 44500$  Hz.

### 6.5.2 Exact Error

Here exact error was calculated with number of modes, procedure is same as first case.

Using (5.8) we can write the *exact* error

$$E = Q(\hat{x}) - Q(\hat{x}_R) = Q(\hat{e})$$

where  $Q(\hat{x})$  is displacement in y direction

Relative error is given by

$$Er = \frac{Q(\hat{x}) - Q(\hat{x}_R)}{Q(\hat{x})}$$

### 6.5.3 Error estimation

Error estimation was done using the same procedure as stated earlier. Exact error in calculating  $u_y$  is plotted in figures 6.20-6.22 for three different forcing frequencies.

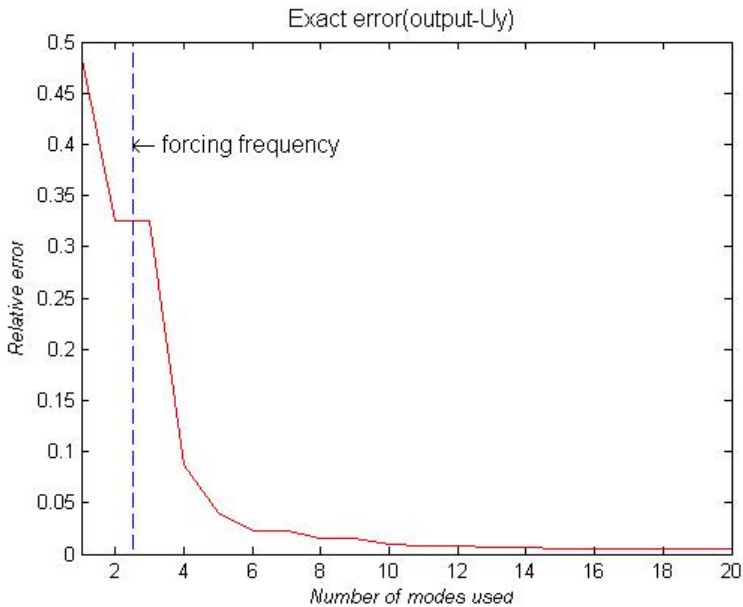


Figure 6.20. Exact error with number of modes,  $f = 800$  Hz, Output- $U_y$ .

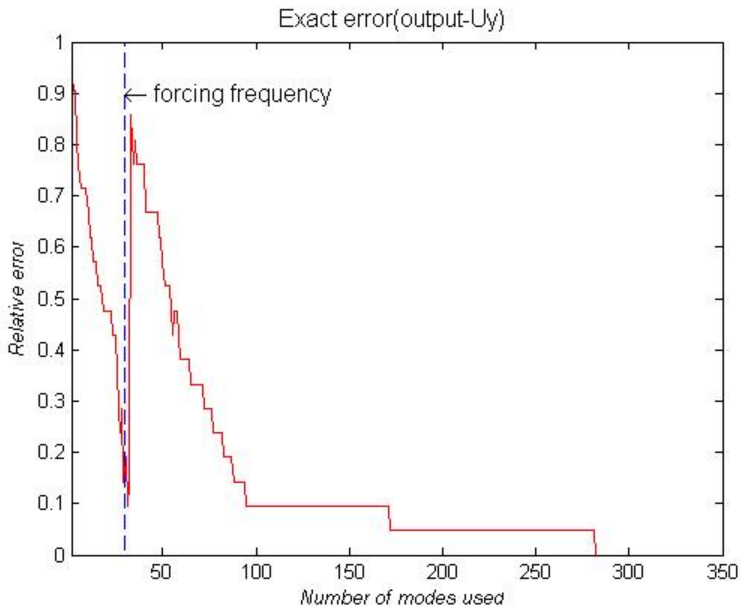


Figure 6.21. Exact error with number of modes,  $f = 22500$  Hz, Output- $U_y$ .

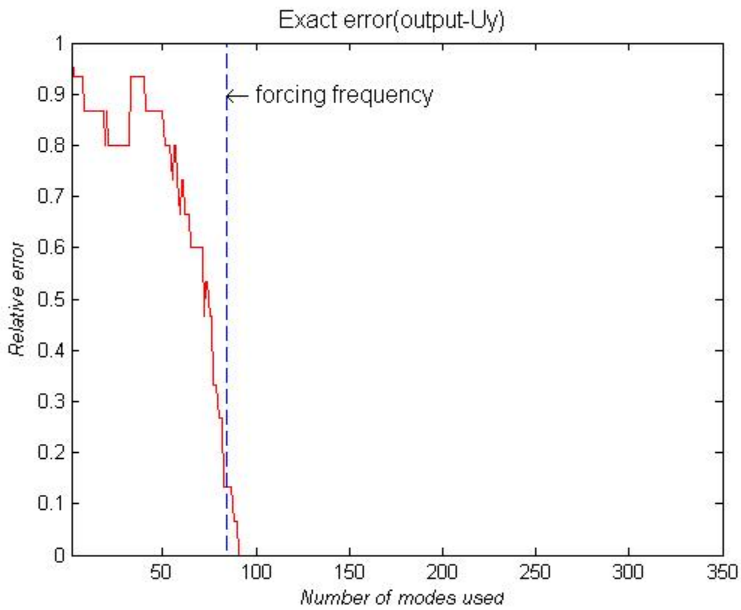


Figure 6.22. Exact error with number of modes,  $f = 44500$  Hz, Output- $U_y$ .

### 6.5.4 Error contribution

The estimated error contribution by each mode is shown in figures 6.23-6.25.

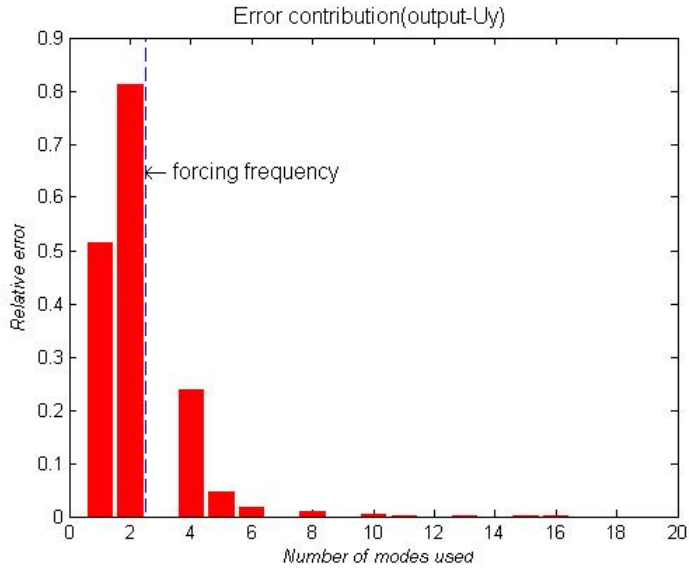


Figure 6.23. Estimated error contribution,  $f = 800$  Hz, output  $U_y$ .

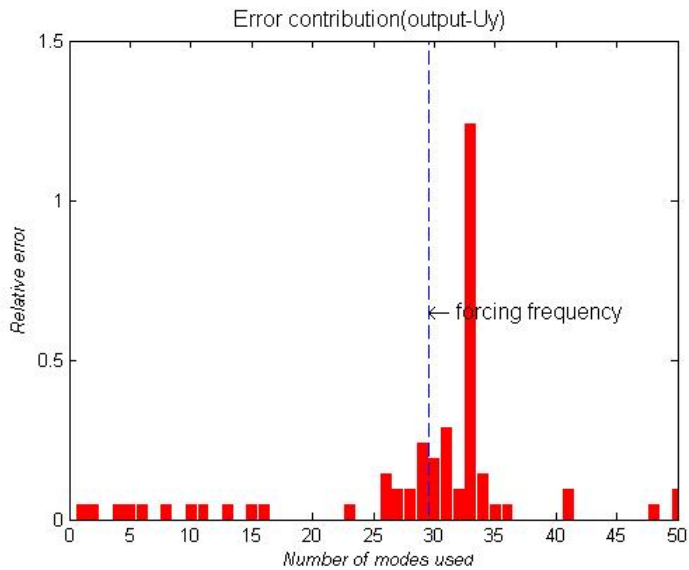


Figure 6.24. Estimated error contribution,  $f = 22500$  Hz, output  $U_y$ .

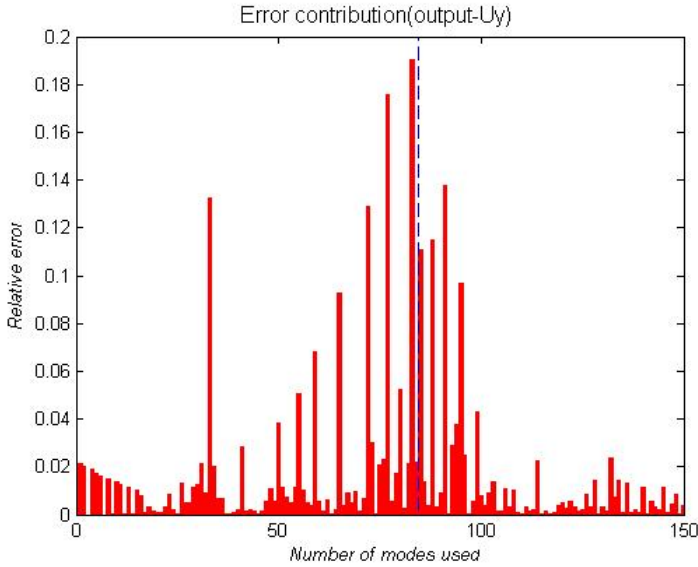


Figure 6.25. Estimated error contribution,  $f = 44500$  Hz, output  $U_y$ .

## 6.6 In plane stress $\sigma_{xx}$

Here we study the errors in calculation in plane stress  $\sigma_{xx}$  direction. Output point is mid span of the beam. All the results are presented in  $\text{N}/\text{mm}^2$ .

### 6.6.1 Dual problem solution

From equation (5.9) we can write dual problem as

$$\underline{Z}(\omega^T) \hat{\underline{x}}^* = \underline{q}$$

where  $\hat{\underline{x}}^*$  vector of size is  $(n \times 1)$  represents the dual displacement,  $\underline{q}$  is the vector generated for output  $u_x$ . Dual displacement is shown in figures 6.26-6.28 for three forcing frequencies

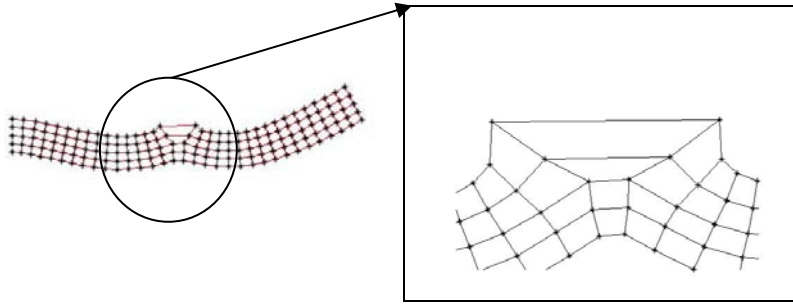


Figure 6.26. Dual displacement  $Re \{ \hat{x}^* \}$ ,  $f = 800 \text{ Hz}$ .

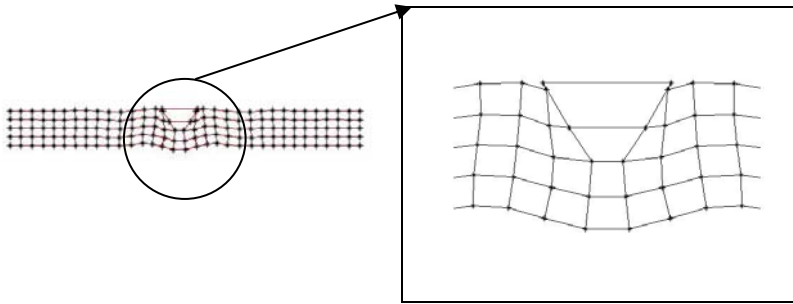


Figure 6.27. Dual displacement  $Re \{ \hat{x}^* \}$ ,  $f = 22500 \text{ Hz}$ .

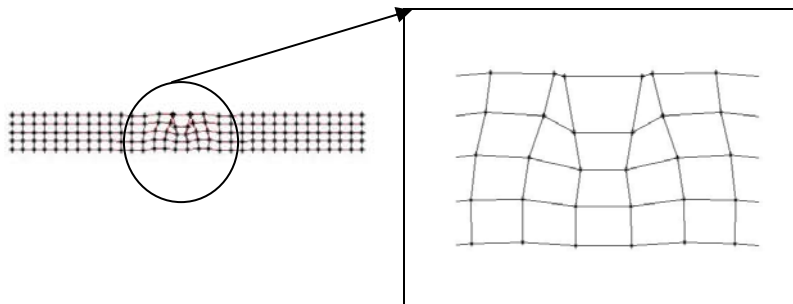


Figure 6.28. Dual displacement  $Re \{ \hat{x}^* \}$ ,  $f = 44500 \text{ Hz}$ .

### 6.6.2 Exact Error

Here exact error was calculated with number of modes, procedure is same as the first case. Using (5.8) we can write the *exact* error

$$E = Q(\hat{x}) - Q(\hat{x}_R) = Q(\hat{e})$$

where  $Q(\hat{x})$  is the displacement in y direction.

### 6.6.3 Error estimation

Error estimation was done using the same procedure as stated earlier. Exact error in calculating  $\sigma_{xx}$  is plotted in figures 6.29-6.31 for three different forcing frequencies.

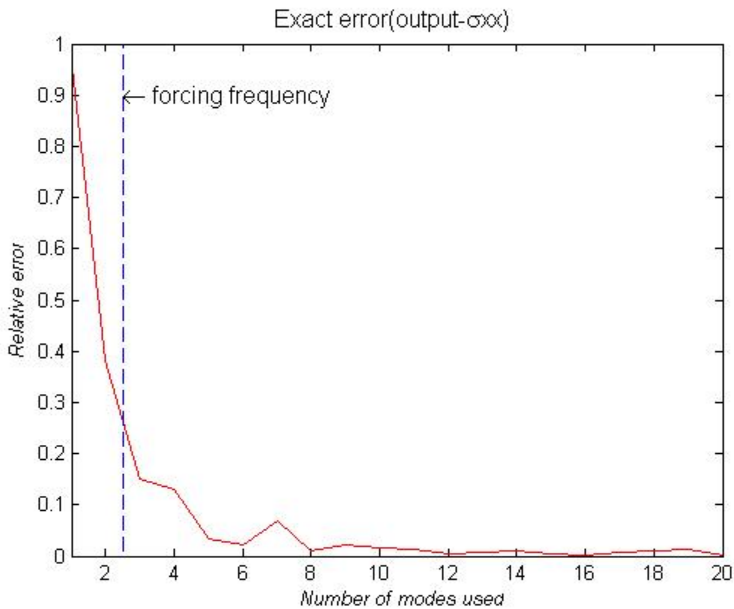


Figure 6.29. Exact error with number of modes,  $f = 800$  Hz, Output  $\sigma_{xx}$ .

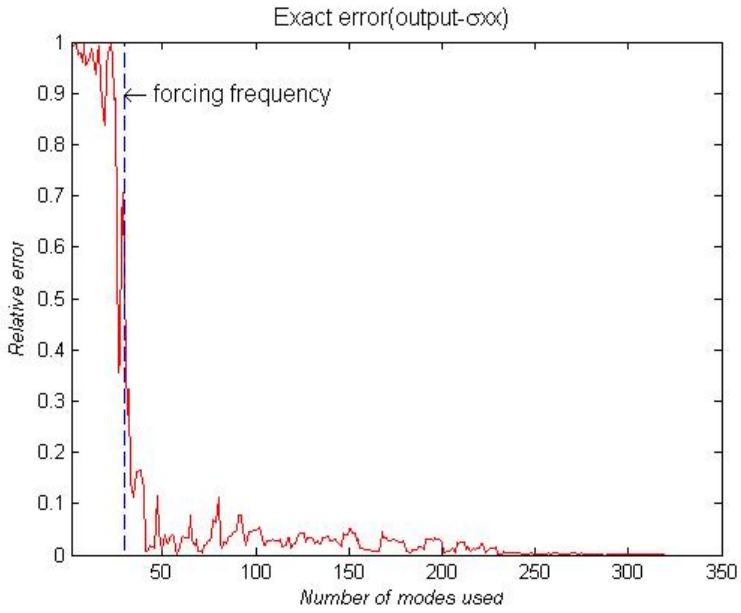


Figure 6.30. Exact error with number of modes,  $f = 22500$  Hz, Output  $\sigma_{xx}$ .

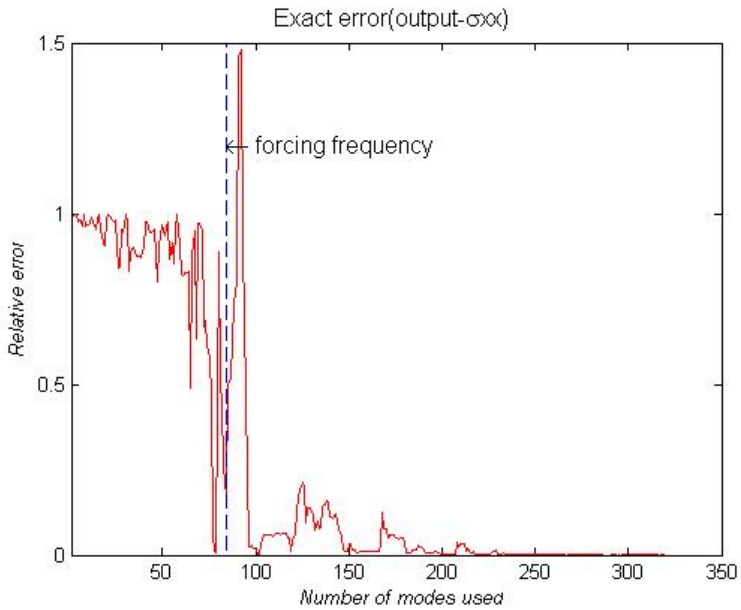


Figure 6.31. Exact error with number of modes,  $f = 44500$  Hz, Output  $\sigma_{xx}$ .

### 6.6.4 Error contribution

The estimated error contribution by each mode is shown in figures 6.32-6.34.

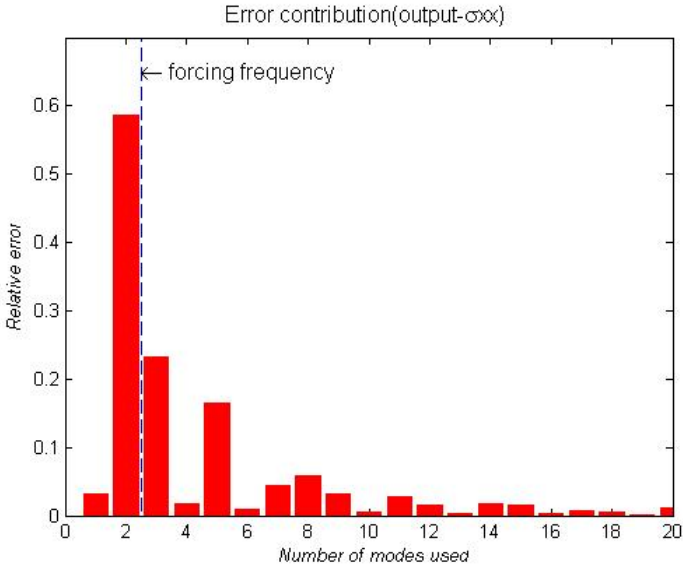


Figure 6.32. Estimated error contribution,  $f = 800$  Hz, output  $\sigma_{xx}$ .

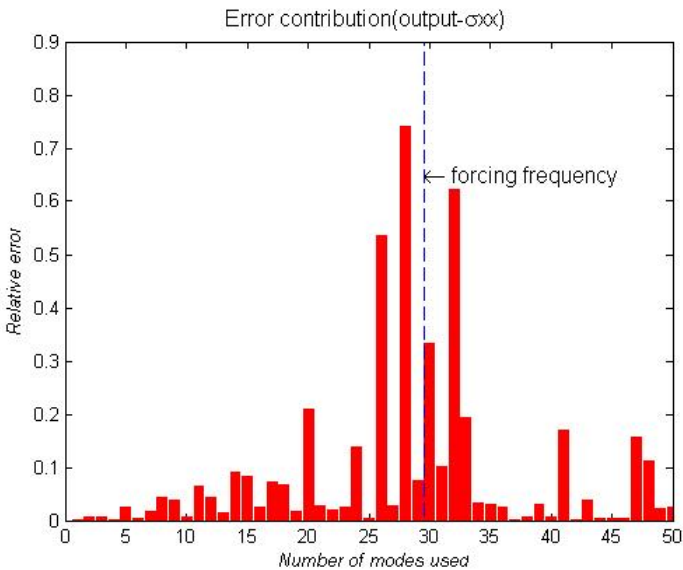


Figure 6.33. Estimated error contribution,  $f = 22500$  Hz, output  $\sigma_{xx}$ .

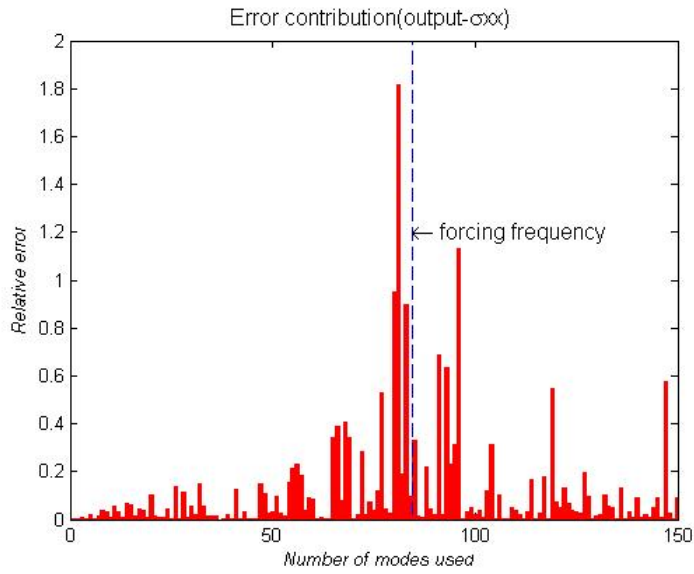


Figure 6.34. Estimated error contribution,  $f = 44500$  Hz, output  $\sigma_{xx}$ .

## 7 Discussions and conclusions

We have adopted a quite general technique for goal oriented error estimation to a reduced basis modal superposition scheme. Restricting the study to a problem of forced harmonic response, error estimations have been derived. As shown in the numerical results (as well as through the derivations themselves) the estimator is exact.

However, it should be noted that estimating the error involves the solution of a dual problem, which is as costly as to solve the ``exact`` unreduced problem itself.

The key advantage of the method is that also the contributions can be obtained, i.e. the estimation relates the error to the individual modes and this indicates which modes need be added for improved accuracy.

In the numerical example, we have taken the three different forcing frequencies and three different output of interest to study for error contributions from the different modes. A careful look at the exact error plots shows drastic reduction in errors near the modes with natural frequencies in the vicinity of the forcing frequencies as expected. This indicates that the modes which are present in the vicinity of excitation frequency are required for accurate result. However; we cannot say that only the modes within the excitation frequency range are the required ones. From the results presented, we see that even modes which are far from the excitation frequency range may have significant influence on the output. Identifying all these modes and using them in a calculation, will lead to further reduction in the computational effort required.

In general, we may conclude that whether or not a mode is relevant for the results depends on three factors; the frequency, load and chosen output functions. Classical methods for adding modes are based only on the frequency, while the proposed strategy allows for taking all factors into account.

## 8 Future work

The work carried so far constitutes the basis for the method. In order to utilise the error estimation technique to increase the efficiency of modal reduction methods, further approximations need be considered.

First of all, the dual solution is as expensive to solve as the unreduced /original problem itself. In order to gain efficiency, an approximate dual solution need be computed, resulting in approximate error estimation.

Secondly, it should be noted that the fully diagonal system studied so far is extremely efficient as such. For more involved problems, that are not possible to diagonalize, the proposed method will add substantially to the efficiency. Examples of such engineering interest are mixed reduction like the Craig-bampton method, non-proportional damping and non-linear problems.

The last and the remaining part of the thesis will deal with error estimation for problems with unproportional damping based on the solution of an approximate dual solution.

Finally, the method supplies the basis for developing adaptive technologies, choosing automatically the optimal set of modes for a certain problem. This is, however, outside the scope of this thesis.

## 9 References

1. Cook, R. D., Malkus, D. S., Plesha, M .E. and Witt, R. J., (2002), Concepts and applications of Finite Element Analysis, 4th ed, John Wiley's and sons.
2. Craig, R. R. Jr., (1981), Structural Dynamics: An introduction to Computer methods, John Wiley's and sons.
3. Clough, R.W. and Penzien, J., (1975), Dynamics of structures, McGraw-Hill.
4. Fertis, D.G.,(1994), Mechanical and structural vibrations ,John Wiley's and sons.
5. Kwon, Y.W. and Bang, H.,(2000), Finite Element using Matlab ,2nd ed , CRC Mechanical series.
6. Kelly, S. G. (1996), Schaum's outline of theory and problems of mechanical engineering, McGraw-Hill, NY.







---

Department of Mechanical Engineering, Master's Degree Programme  
Blekinge Institute of Technology, Campus Gräsvik  
SE-371 79 Karlskrona, SWEDEN

Telephone: +46 455-38 55 10  
Fax: +46 455-38 55 07  
E-mail: [ansel.berghuvud@bth.se](mailto:ansel.berghuvud@bth.se)